

Article

# Controlling the Polymorphic Outcome of 2,6-Dimethoxybenzoic Acid Crystallization Using Additives

Aina Semjonova \* and Agris Bērziņš 

Faculty of Chemistry, University of Latvia, Jelgavas iela 1, LV-1004 Rīga, Latvia

\* Correspondence: aina.semjonova@lu.lv

**Abstract:** In this study, 2,6-dimethoxybenzoic acid (2,6MeOBA) was used as a model substance to investigate the use of additives to control the polymorphic outcome of crystallization. 2,6MeOBA exists as three polymorphs. Two of the 2,6MeOBA polymorphs, I and III, obtained in most of the crystallization experiments, were characterized by thermal analysis, and their relative thermodynamic stability was determined. Forms I and III are enantiotropically related, where form III is the high-temperature form. Pure form II was very difficult to obtain. Crystallization of 2,6MeOBA was explored under different conditions by performing evaporation and cooling crystallization from different solvents. Surfactants, polymers, and different molecular compounds with diverse possibilities for the formation of intermolecular interactions were tested as additives. The additives facilitating the crystallization of the metastable forms were additionally studied under different crystallization conditions. The effect of additives polyethylene glycol (PEG) and hydroxypropyl cellulose (HPC) on the thermodynamic stability and solvent-mediated phase transition (SMPT) kinetics was evaluated. HPC and PEG showed the potential to favor the formation of form III in crystallization from water.

**Keywords:** 2,6-dimethoxybenzoic acid; polymorphism; crystallization; crystallization additives; solvent-mediated phase transition



**Citation:** Semjonova, A.; Bērziņš, A. Controlling the Polymorphic Outcome of 2,6-Dimethoxybenzoic Acid Crystallization Using Additives. *Crystals* **2022**, *12*, 1161. <https://doi.org/10.3390/cryst12081161>

Academic Editor: Klaus Merz

Received: 19 July 2022

Accepted: 15 August 2022

Published: 18 August 2022

**Publisher's Note:** MDPI stays neutral with regard to jurisdictional claims in published maps and institutional affiliations.



**Copyright:** © 2022 by the authors. Licensee MDPI, Basel, Switzerland. This article is an open access article distributed under the terms and conditions of the Creative Commons Attribution (CC BY) license (<https://creativecommons.org/licenses/by/4.0/>).

## 1. Introduction

Polymorphism is the ability of compounds to crystallize in different solid crystal structures [1,2]. It is often one of the most challenging steps in the development of pharmaceutical drugs [3–5]. Polymorphism and its control possibilities are not completely predictable, despite extensive research in this field. As polymorphs are also considered intellectual property, pharmaceutical companies often patent-protect the discovered crystalline forms [6,7]. A general understanding of the mechanism of polymorph formation can reduce the research and development time for the invention of new active substances or generic drugs [8]. For a better understanding of the phenomenon of polymorphism and factors affecting their appearance and crystallization, well-explored or specifically selected model substances are often used for research.

Solids with different crystal structures have different physical properties, for example, solubility [9], dissolution rate [10], stability [11], and bioavailability [12,13]. It is important to characterize all crystalline forms of API before developing the dosage form of the drug [14,15] because the selection of the dosage form, required excipients, and dose of the API depends on these physical properties [16]. In pharmaceutical manufacturing, it is safer to use the most stable polymorph with the lowest energy, but many APIs have low solubility in water. Crystallization of metastable forms improves solubility and bioavailability [17]. Unfortunately, the crystallization of such polymorphs is often complicated, with concomitant crystallization along with the stable form being one of the potential complications [18–20].

Concomitant crystallization occurs when at least two different polymorphs crystallize in the same sample [20]. This can occur due to competitive nucleation and growth rates of

more than one polymorph [21]. The appearance of concomitant crystallization is caused by different kinetic and thermodynamic factors [22,23]. Frequently, a mixture of forms is exposed to a solvent-mediated phase transition (SMPT), and only the stable form is present in the collected product [18,21,24,25]. Modification of the crystallization process can prevent concomitant crystallization. One such modification is the use of crystallization additives, which can stabilize metastable forms [26–28], promote their nucleation [29], or prevent nucleation of the stable form.

Crystallization with the presence of additives or templates is one of the empirical methods for controlling polymorphic outcomes. There are many approaches to additive crystallization [30]—heterogeneous nucleation with insoluble additives or templates (for example, Langmuir monolayers [31,32], self-assembled monolayers (SAM) [23,33–35], polymers [24,36,37], or other insoluble additives [38]) or homogeneous nucleation with soluble additives [29,37]. Additives typically lower the activation energy of nucleation and control crystal morphology, polymorphism, and crystal size [23]. Langmuir monolayers and SAMs are efficient templates for crystallization control but are selective for each polymorph, it is necessary to regenerate the monolayers after crystallization, or it is difficult to collect the obtained crystals without impurities from the layers [39]. Homogeneous additives can be easier to separate from the crystals but sometimes integrate into the crystal structure [29]. Therefore, excipients from drug dosage forms can be used as additives for the crystallization of API [37,40], as there would be no need to separate these additives after crystallization. There are many possible mechanisms by which additives can control the outcomes of crystallization. For example, additives can selectively adsorb to some of the crystal surface faces by inhibiting their growth and, therefore, the growth of this polymorph. Additives can also help to align crystallizable substance molecules to obtain the desired polymorph [28,30,32,37,41]. However, the exact mechanism for the control mechanism by additives in most cases is still unknown.

Here, we report a study of polymorphs and crystallization of 2,6-dimethoxybenzoic acid (2,6MeOBA). 2,6MeOBA has been reported to crystallize in three polymorphic forms [42–46]. Form I is the stable polymorphic form [45,46]. Metastable polymorphs II and III, in previous studies, were described as disappearing polymorphs [45,46]. In this study, we explore the relative stability of 2,6MeOBA polymorphs and the ability of additives to alter the polymorphic outcome of its crystallization. 2,6MeOBA was selected for this study because of two factors. First, the two distinct hydrogen bonding patterns present in the stable and metastable polymorphs could more easily allow the additives to alter the polymorphic outcome of crystallization. Second, we selected this compound to try to find an approach for additive crystallization that would allow a reliable preparation procedure for the disappearing polymorphs. Our previous study [47] has already confirmed that polymorphs II and III can be obtained by varying the crystallization conditions. In this study, we additionally characterized forms I and III, performed screening of additives allowing control of the polymorphic outcome in the crystallization, explored the most promising additives for the crystallization control, and explored the effect of additives on phase transitions.

## 2. Materials and Methods

2,6-dimethoxybenzoic acid (2,6MeOBA) (purity 99%, polymorph I), polyethylene glycol (PEG, MW = 6000), and hydroxypropyl cellulose (HPC, MW = 100,000) were purchased from Alfa Aesar. 2,6-dimethoxybenzoic boronic acid (2,6MeOPheBorA) (purity 97%) was purchased from Fluorochem. The molecular structures of 2,6MeOBA and selected additives are shown in Figure 1. The water was deionized in the laboratory. Other additives (see Supplementary Materials, Table S1) and analytical grade organic solvents were purchased from commercial sources.

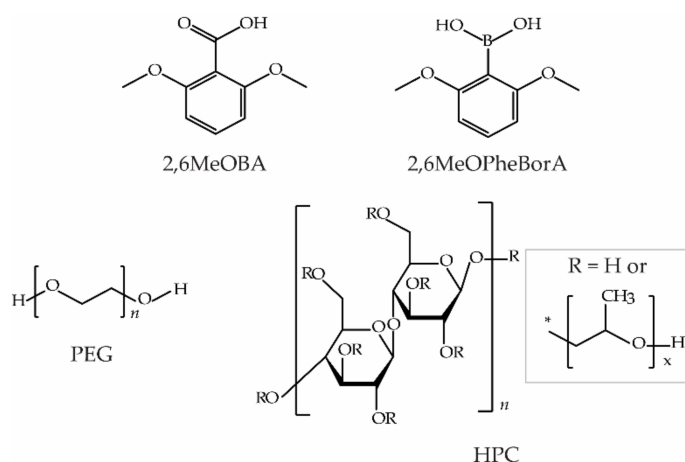


**Figure 1.** Molecular structure of 2,6MeOBA, 2,6MeOPheBorA, PEG, and HPC.

### 2.1. Crystallization Experiments

Several widely used solvents from different solvent classes were selected for the polymorph screening of 2,6MeOBA. For evaporation crystallization, 30–50 mg of 2,6MeOBA were dissolved in 2 to 3 mL of solvent and evaporated at 5, 25, and 50 °C. For cooling crystallization, 2,6MeOBA was dissolved in a selected solvent at 40 to 80 °C, depending on the boiling point of the solvent. The solutions obtained were filtered and cooled to 5 °C. The obtained products were collected by filtration, air-dried, and characterized with PXRD. Tetrahydrofuran (THF), acetonitrile (MeCN), and water were selected for the screening of additives, allowing control of crystallization polymorphic outcome.

Crystallization in the presence of additives in THF and MeCN was performed as a complete solvent evaporation. In 2 to 3 mL of solvent, 20 to 30 mg of additive and 30 to 50 mg of 2,6MeOBA were dissolved, and the solution was filtered and evaporated at room temperature. Crystallization in the presence of additives in water was performed as cooling crystallization. In 3–4 mL of water at 80 °C, 10–15 mg of additive and 20–25 mg of 2,6MeOBA were dissolved, filtered, and cooled to 5 °C. Three parallel crystallization experiments were performed for each additive. The products obtained were collected by filtration, air-dried, and characterized with PXRD.

Further cooling crystallization experiments were performed using *Crystal16* (Technobis). Of all additives tested, three additives (2,6MeOPheBorA, PEG, HPC) were selected for these additional studies. Highly concentrated solutions (having supersaturation  $c/c^* \approx 9$  at 25 °C) of 2,6MeOBA were made. A concentrated solution of 2,6MeOBA was prepared in the 50 mL flask of water equipped with an air reflux condenser. The solution was prepared by boiling and stirring for 2 to 3 h. The identical preparation process was used for solutions with additives using ~0.1 wt % HPC, 1 wt % PEG, or 0.5 wt % 2,6MeOPheBorA (the concentration given with respect to the water added). After boiling, the solution was stored at 90 °C and filtered. Then, 1 mL of the sample was transferred to preheated HPLC vial, which was placed in *Crystal16* preheated to 90 °C and then cooled to 10 °C with different cooling rates—20, 10, 1, and 0.1 °C·min<sup>-1</sup> by using the stirring rate of 900 rpm. Another series of experiments with HPC suspension was prepared in situ in *Crystal16*. HPC has a low critical dissolution temperature of 45 °C [48], which means that at temperatures above 45 °C, it is insoluble in water. The suspension was prepared by using 23–25 mg of 2,6MeOBA ( $c/c^* \approx 7$  at 25 °C) and 0.5 wt % of HPC added to 1 mL of water in an HPLC vial, heated to 90 °C using *Crystal16*, thermostated for 30 min to completely dissolve 2,6MeOBA, and cooled with the same cooling rates by additional stirring. Four parallel crystallization experiments were performed in all cases. The obtained products were collected by filtration, air dried, and characterized with PXRD.

To determine the effect of the amount of additive on the crystallization results, 2,6MeOBA solutions were prepared in situ in *Crystal16*. The additive weight fractions tested were 0.5; 0.7; 1; 1.5, and 2 wt %. HPC solutions were prepared as described above for

the 0.5 wt % solutions. The cooling rate was chosen based on the previous experiments—20 and 10 °C·min<sup>-1</sup>. The solutions containing PEG were prepared by first making aqueous PEG solutions. Subsequently, 33 to 35 mg of 2,6MeOBA ( $c/c^* \approx 10$  at 25 °C) and 1 mL of different concentration PEG solutions were added to the HPLC vial, heated to 90 °C for 30 min in *Crystal16*, and cooled with a cooling rate of 20 and 1 °C·min<sup>-1</sup> by stirring. For each of the different crystallization conditions, blank crystallization experiments without any additive were performed. Each experiment was carried out as four parallel crystallizations. The obtained products were collected by filtration, air dried, and characterized with PXRD.

## 2.2. Solubility Measurements and Solvent-Mediated Phase Transition (SMPT) Studies

For these experiments, the 2,6MeOBA form I from the commercial sample was used as received, the form III was prepared in a phase transition that occurred by heating the form I at 160 °C in the air thermostat for 1 h. The phase purity of both forms was verified with PXRD (Bruker AXS, Karlsruhe, Germany).

Solubility measurements were performed using *Crystal16* (Technobis Crystallization Systems, Alkmaar, Netherlands). From 4 to 34 mg of each 2,6MeOBA polymorph was weighted in an HPLC vial, 1 mL of water or 1 wt % of the aqueous solution of PEG was added, and the mixtures were heated at a heating rate of 0.1 °C·min<sup>-1</sup> from 10 to 90 °C. The stirring rate was 900 rpm. The temperature of dissolution was determined by recording the temperature at which the solution became transparent using turbidity measurements [49]. The experimental dependence of the temperature of solubility was fitted with linear regression and the van't Hoff equation by the least-squares approach using the Microsoft Excel Linest add-in.

To determine the thermodynamic stability of 2,6MeOBA polymorphs at different temperatures, slurry-bridging experiments were performed. Forms I and III with a 1:1 mass ratio were suspended in 1 mL of water, toluene, and aqueous solutions of 0.1 wt % HPC and 1 wt % PEG for 24 h at 25, 50, 70, and 80 °C with a stirring rate of 900 rpm.

The solvent-mediated phase transition kinetics in 2,6MeOBA suspensions in water, isopropanol (IPA), MeCN, and ~0.1 wt % of HPC, and 1 wt % of PEG aqueous solutions were determined at 25 °C. Four experiments in each of the solvents were prepared using a 1:1 ratio (*w/w*) of both polymorphs as well as pure polymorph III. The samples were collected after 15, 30, 45, and 60 min of stirring by filtration, air dried, and characterized with PXRD. Form III in 0.1 wt % HPC solution was suspended for 24 h because no SMPT was observed for 60 min.

## 2.3. Solid Phase Characterization

The PXRD patterns were measured at ambient temperature on a Bruker D8 Advance diffractometer using copper radiation (Cu K $\alpha$ ;  $\lambda = 1.54180 \text{ \AA}$ ), equipped with a LynxEye position-sensitive detector. The tube voltage and current were set to 40 kV and 40 mA, respectively. The divergence slit was set at 0.6 mm. The anti-scatter slit was set at 8.0 mm. The PXRD patterns were recorded from 3° to 35° on the 2  $\theta$  scale. A scan speed of 0.2 s/0.02° was used.

Differential scanning calorimetry/thermogravimetry (DSC/TG) analysis was performed using the Mettler Toledo TGA/DSC 2 (Mettler Toledo, Greifensee, Switzerland). Closed aluminum pans were used. The heating of the samples from 25 to 250 °C was carried out at a heating rate of 10 °C·min<sup>-1</sup>. Samples of 5 to 8 mg mass were used. The nitrogen flow rate was 30 mL·min<sup>-1</sup>.

## 2.4. Rietveld Refinement for Form Quantification

The Rietveld refinement for the quantification of the polymorphs was performed with Profex 4.3.6 (Dobelin, N., Kleeberg, R., Solothurn, Switzerland) [50]. For this analysis, crystal structures of 2,6MeOBA polymorphs were acquired from the CSD with Ref. codes DMOXBA01 (form I), DMOXBA03 (form II), and DMOXBA07 (form III).

### 3. Results and Discussion

#### 3.1. Characterization of 2,6MeOBA Polymorph

2,6MeOBA polymorphs are both conformational polymorphs and synthon polymorphs [44–46]. According to previous investigations, the most stable polymorph is form I, which crystallizes in the orthorhombic space group  $P2_12_12_1$  [42,43] and contains 2,6MeOBA molecules in the *anti*-planar conformation linked by hydrogen-bonded chains that form the catemer synthon (see Figure 2). Both metastable polymorphs form II and form III contain 2,6MeOBA molecules in a *syn*-planar conformation that forms carboxylic acid homodimers [42,43]. Form II crystallizes in the tetragonal space group  $P4_12_12$  [44]. After various screenings and additive experiments performed as part of this study, pure form II was never obtained, suggesting that it is the least stable 2,6MeOBA polymorph. Form III crystallizes in the monoclinic centrosymmetric space group  $P2_1/c$  [45,46].

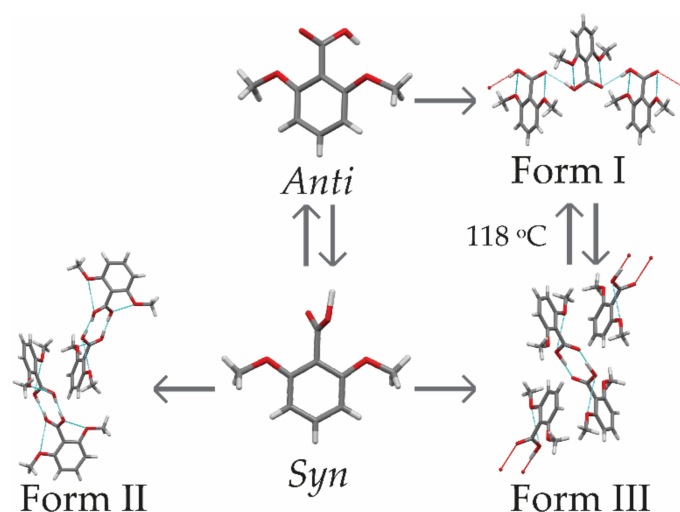


**Figure 2.** Relationships between 2,6MeOBA conformations and polymorphs. The connection between forms I and III is elucidated in this study.

##### 3.1.1. Thermal Characterization and Solubility

In the DSC, traces of form I two endothermic events can be observed (see Figure 3). The peak onset at 118 °C corresponds to a phase transition of form I to form III, as confirmed by the PXRD analysis, while the second is the melting of form III. Form I and form III are enantiotropically related by the heat-of-transition rule [51], as the phase transition is endothermic. The melting point onset of form III is 190 °C. There is no change in the TG curves for any of these forms, except for the decomposition that occurs above 200 °C.

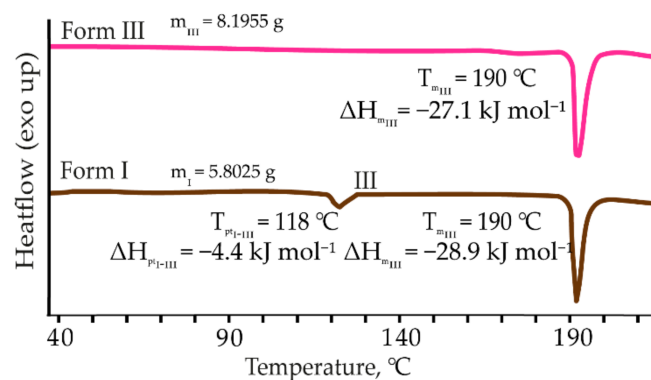


**Figure 3.** DSC curves of 2,6MeOBA polymorphs I and III (heating rate 10 °C·min<sup>-1</sup>). The onset temperatures were used to describe each process observed in the DSC traces.

The solubility of forms I and III in water shows that form I is the stable polymorph (as determined from the lower solubility) at temperatures up to 79 °C (see Figure 4). At ambient temperature, the solubility of form III is 1.3 times higher than that of form I. Form III becomes the most stable polymorph above 79 °C. The theoretical solubility temperature dependence lines for each polymorph were obtained by fitting the natural logarithm of obtained solubility ( $\ln S$ , where  $S$  in  $\text{mg mL}^{-1}$ ) and the inverse of temperature ( $1/T$ , where  $T$  in K) to the van't Hoff Equation (1):

$$\ln S = \frac{a}{T} + b \quad (1)$$

**Table 1.** Coefficients of the van't Hoff equation for solubility curves of 2,6MeOBA polymorphs in pure water.

Polymorph	a	b	R <sup>2</sup>	SE for $\ln S_{\text{calc}}$
I	$-3960 \pm 130$	$15 \pm 0.4$	0.9894	0.09
III	$-3400 \pm 110$	$13 \pm 0.3$	0.9909	0.08

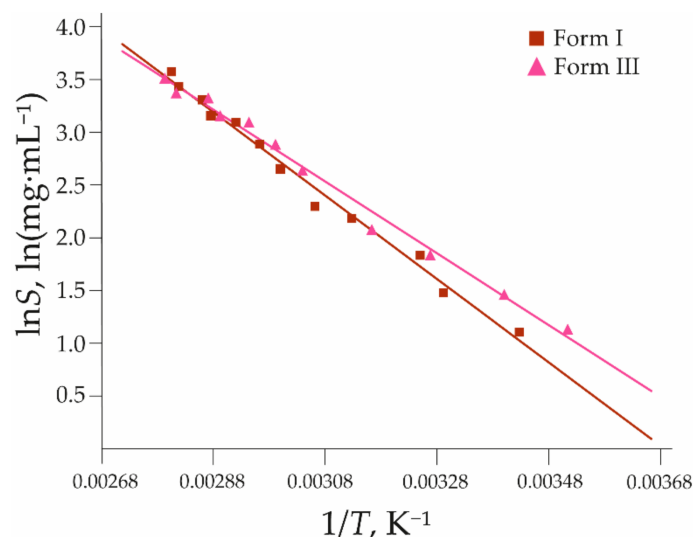


**Figure 4.** The solubility of 2,6MeOBA polymorphs I and III. Squares and triangles represent experimental data (see Supplementary Materials Tables S2 and S3), while lines are calculated using Equation (1) with coefficients  $a$  and  $b$  found in the fitting using the least-squares approach, given in Table 1.

### 3.1.2. Solvent-Mediated Phase Transition (SMPT)

The thermodynamic stability determined using slurry-bridging experiments at different temperatures agrees with the results obtained in the DSC/TG analysis and from the solubility curves. After 24 h, pure form I was obtained in water and toluene by suspending a mixture of both forms at 25, 50, and 70 °C. However, form III was obtained in both solvents at a temperature of 80 °C. These results confirm that the solubility curves of both forms cross between 70 and 80 °C.

Measurements of solvent-mediated phase transition kinetics show that the transformation rate in the slurry-bridging experiments is very fast (see Figure 5). Pure form I was obtained in less than 15 min at 25 °C in the mixture of both forms in the three solvents tested. The complete transformation of pure form III to pure form I in IPA and MeCN occurred as fast as from the polymorph mixture, but in water, it is slower and requires between 15 and 30 min. This can be explained by the lower solubility of 2,6MeOBA in water or the better possibilities of hydrogen bonding with water for 2,6MeOBA in *syn* conformation.

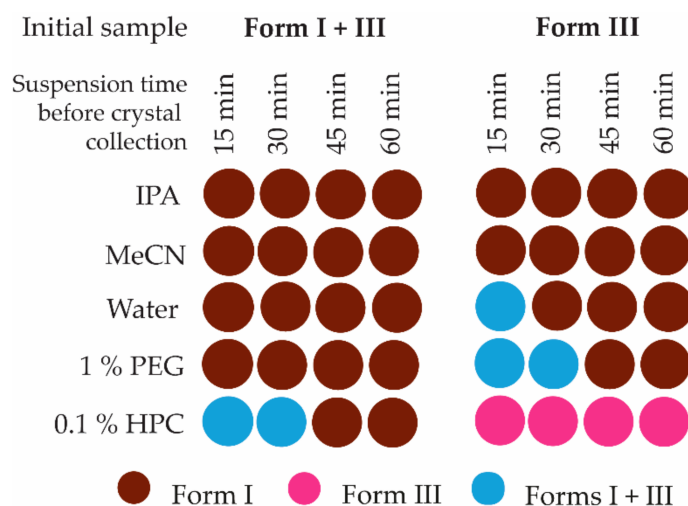


**Figure 5.** Polymorphic composition of the solid phase after selected times during SMPT kinetic experiments at 25 °C.

### 3.2. Crystallization from Pure Solvents

In most cases of the cooling crystallization, form I was obtained, although impurity of form III was sometimes present. The polymorph obtained correlated with the temperature in the evaporation crystallization experiments: at lower temperatures (5 °C) in most of the experiments, form I was obtained, frequently with some impurities of form III. However, at higher temperatures (50 °C), the polymorphic outcome is the opposite. The thermodynamic equilibrium point is rather close to 50 °C; therefore, form III is more likely to be obtained compared to evaporation at 5 °C. 1,4-dioxane, MeCN, and ketones can be used as solvents to obtain form III by evaporation, but these are not selective solvents. Water was the only solvent from which form I was obtained in almost all crystallizations. Using these preliminary crystallization experiments, three solvents were selected for crystallization experiments in the presence of additives: MeCN, THF, and water. The results of the crystallization experiments from pure solvents with phase composition of samples containing polymorph mixtures obtained using the Rietveld analysis are given in the supporting information, Table S4 and Figure S2.

### 3.3. Crystallization with Additives

The additives selected for the crystallization were polymers and surfactants that have the ability to form different intermolecular interactions. The polymorphic outcome of the crystallization in the presence of the selected additives was the same in most cases as that in crystallization from a pure solvent. From THF, some of the additives resulted in the crystallization of form III, whereas tween 20 promoted the formation of form I in all three parallel samples (see Figure 6, detailed results can be seen in Table S5). This additive was not further studied because the study aimed to find an approach for crystallization of the metastable form. Additives facilitated the concomitant crystallization of forms I and III from MeCN. Despite the very low solubility, polyvinyl chloride promoted the crystallization of form I. Overall, it can be concluded that the outcome of the evaporation crystallization from these solvents is difficult to control, even in the presence of the selected additives.

Repeated crystallizations from pure water with immediate filtration and analysis of the obtained crystals confirmed that a mixture of forms I and III crystallizes, followed by a solvent-mediated phase transition in the case that the crystals remain in suspension (see Figure 6). Therefore, only form I was observed in the preliminary crystallization experiments. Phenylboronic acid and several of its derivatives were tested as additives in crystallization from water because it was used as an additive to crystallize form II in one of the previous studies [44]. Concomitant crystallization of forms I and III or the stable form I was observed using several of the tested additives, including phenylboronic acid,

4-iodophenylboronic acid, and 4-carboxyphenylboronic acid. Some of the additives (e.g., BIS-TRIS, PEG) facilitated the formation of form II in a mixture with other polymorphs. All three crystallizations in the presence of HPC occurred very fast and produced form III. Almost the same crystallization rate was observed in the presence of 2,6MeOPheBorA, but the crystallization product was form III with minor impurities of form I. Crystallization in the presence of PEG was slower than in the presence of HPC and 2,6MeOPheBorA, but also, in this case, in two of the crystallizations, pure form III was obtained, although in the third crystallization, a mixture of all three polymorphs was formed. Additionally, form III was obtained in crystallization from THF in the presence of PEG in two of three experiments. Based on the results obtained, HPC, 2,6MeOPheBorA, and PEG were chosen for more detailed studies.

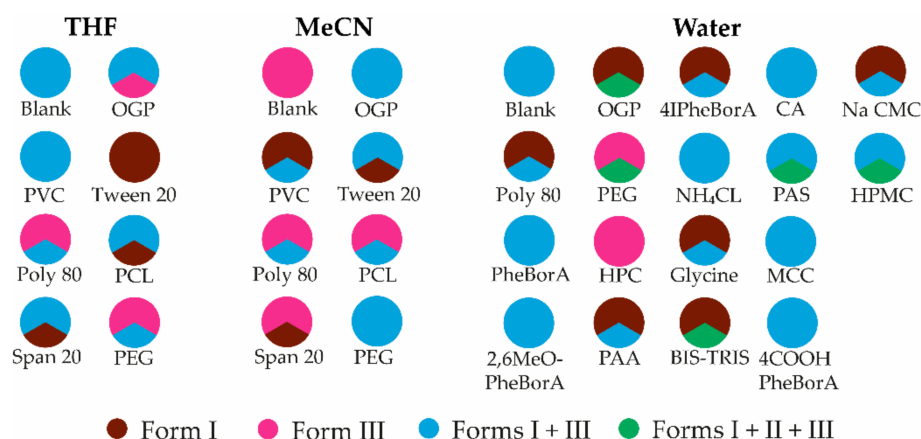


**Figure 6.** Polymorphic outcome of crystallization experiments in the presence of additives from THF, MeCN, and water. Each 1/3 of the pie chart represents one of the parallel experiments.

### 3.3.1. Crystallization from Highly Concentrated Water Solution

Highly concentrated 2,6MeOBA water solutions were used for these experiments to understand the additive effect on the crystallization of concentrated solutions. Mixtures of three polymorphs were obtained in crystallization from a highly concentrated pure water solution with the fastest cooling rate of  $20\text{ }^{\circ}\text{C}\cdot\text{min}^{-1}$  (see Figure 7, column A). This result agrees with Ostwald's rule of stages [52]: instead of the nucleation of the most stable form, the polymorph corresponding to the nearest minimum energy nucleates. Two different polymorph mixtures were obtained at a cooling rate of  $10\text{ }^{\circ}\text{C}\cdot\text{min}^{-1}$ . A medium cooling rate resulted in the formation of a mixture of forms I and III. The cooling rate needs to be fast to obtain form II, but such an approach cannot prevent concomitant crystallization with other forms. Additionally, form II very rapidly transforms into more stable forms. Supersaturation can also play an important role in obtaining unstable polymorphs [53,54]. A higher concentration of 2,6MeOBA was used for samples cooled with a specific cooling rate compared to the preliminary crystallization experiments from pure solvents. Nevertheless, the effect of supersaturation on the polymorphic outcome was not examined. The four samples with the lowest cooling rate ( $0.1\text{ }^{\circ}\text{C}\cdot\text{min}^{-1}$ ) produced form III; however, at a slower cooling rate, the formation of the thermodynamically stable form I was expected. In these experiments, the crystals appeared at approximately  $60\text{ }^{\circ}\text{C}$ , which is rather closer to the thermodynamical equilibrium point of forms I and III. The crystals appeared at lower temperatures ( $40\text{--}50\text{ }^{\circ}\text{C}$ ) in crystallizations using faster cooling rates. The phase transition to form I was prevented as the crystals formed near the water surface and formed large agglomerates. In contrast, the crystals in the SMPT kinetics experiments and in the case of using faster cooling rates were smaller and evenly suspended in the solution. Using PEG (see Figure 7, column B, detailed results can be seen in Table S6) and 2,6MeOPheBorA (see Figure 7, column C) as additives and 2,6MeOBA solution with a concentration corresponding to  $c/c^* \approx 9$  at  $25\text{ }^{\circ}\text{C}$ , a mixture of forms I and III was obtained in most of the crystallizations. In contrast, using HPC as an additive (see Figure 7, columns D and E) at

both additive concentrations, pure form III was the most frequent crystallization product. The formation of form III was facilitated by the fastest cooling rates (20 and 10 °C·min<sup>-1</sup>). On the contrary, under the same conditions as those of pure water, concomitant crystallization of 2,6MeOBA polymorphs always occurred. Interestingly, at the slowest cooling rate (0.1 °C·min<sup>-1</sup>), additives promoted crystallization of form I. Using 0.5% HPC suspension and 2,6MeOBA solution with lower concentration (corresponding to  $c/c^* \approx 7$  at 25 °C), crystallization of form III is promoted more clearly if compared to crystallization from 0.1% HPC solution and a higher concentration of 2,6MeOBA (corresponding to  $c/c^* \approx 9$  at 25 °C). It is possible that more HPC molecules can interact with 2,6MeOBA in heterogeneous crystallization and stabilize the *syn* conformation during nucleation, similar to the research by Lin et al. studying the crystallization of  $\alpha,\omega$ -alkanedicarboxylic acids [55]. Lin et al. [55] developed a method to control the crystallization outcome for conformation polymorphs having similar structures. The desired polymorph was crystallized on the template lattice, where dimer formation was possible. An additional explanation for why the crystallization control in homogeneous 0.1% HPC solution is not so effective can be the higher supersaturation; there are more 2,6MeOBA molecules but fewer HPC molecules, which apparently provide formation of form III. PEG also has the potential to control the crystallization outcome in the case of a moderately slow cooling rate (1 °C·min<sup>-1</sup>) from a highly concentrated solution. It is possible that the additives slow down the phase transition to form I, which can initiate right after the nucleation, but not enough to obtain pure form III, as stirring is still employed after the nucleation. The phase transition time can, in fact, be reduced as the crystal sizes obtained in additive crystallization are smaller than those obtained in crystallization from pure water. In general, the tested additives do not provide fully selective crystallization control. Nevertheless, PEG and HPC under multiple conditions distinctly favor the formation of form III, whereas, under the tested conditions, 2,6MeOPheBorA still provided a mixture of 2,6MeOBA polymorphs. Crystallizations in the presence of PEG with a cooling rate of 20 and 1 °C·min<sup>-1</sup> and in the presence of HPC with 20 and 10 °C·min<sup>-1</sup> were selected for further study to test the effect of the amount of additive on the crystallization result.

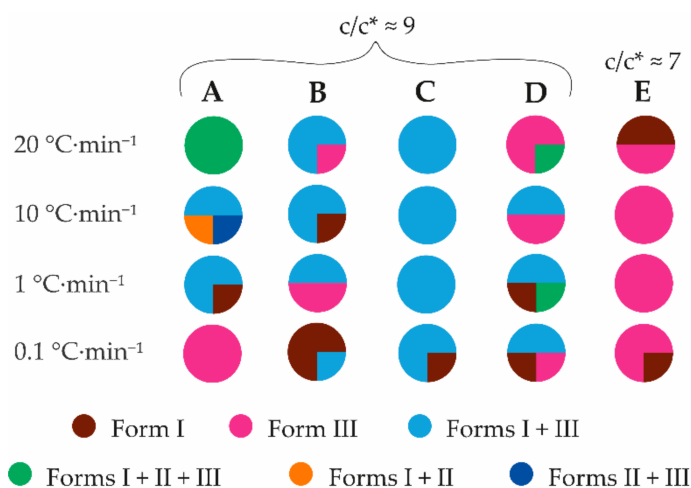


**Figure 7.** Polymorphic outcome of the crystallization experiments from water using different additives and cooling rates. A—pure water; B—1% PEG; C—0.5% 2,6MeOPheBorA; D—0.1% HPC; E—heterogeneous crystallization using 0.5% HPC.

### 3.3.2. The Effect of the Additive Quantity on the Crystallization Outcome

From pure water using the slowest cooling rate in most of the crystallizations, form I was obtained, but a mixture of forms I and III or the stable form I was obtained using the fastest cooling rate (see Figure 8, detailed results can be seen in Table S7). Form III was obtained in most of the crystallizations using both additives and the fastest cooling rate. Again, the presence of additives did not provide selective crystallization of either of

the polymorphs. Concomitant crystallization of both polymorphs was less frequent in the presence of HPC than in the presence of PEG. No clear correlation was observed between the amount of additive selected and the crystallization outcome. It is likely that additives decrease the interfacial energy and, therefore, lower the nucleation Gibbs energy, facilitating the crystallization of form III from this solution compared to the pure water solution.

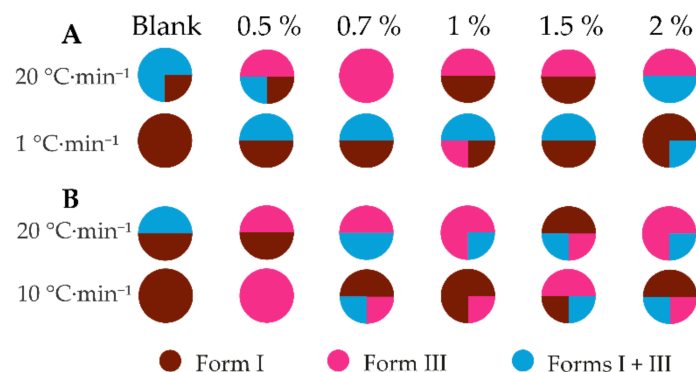


**Figure 8.** Polymorphic outcome of the crystallization experiments from water in the presence of different quantities of (A) PEG and (B) HPC.

### 3.4. Effect of Additives on Polymorph Solubility and Solvent-Mediated Phase Transitions

The solubility of form I is almost unaffected by the addition of 1% PEG (see Figure 9). At temperatures up to 30 °C, the solubility is almost identical to that in pure water, but at higher temperatures, the solubility slightly decreased. In contrast, the solubility of form III in the presence of PEG increases slightly at temperatures up to 35 °C, but the solubility at higher temperatures is lower than in the pure solvent. As the PEG solution separated into two phases above 75 °C, the solubility in this solution cannot be determined above this temperature. Additives have been shown to affect the solubility and crystal growth of organic compounds in the literature. For example, additives have been demonstrated to decrease the solubility but increase the crystal nucleation and growth rates of *p*-methylacetanilide [56]. The highly similar solubility of both forms can explain the nearly always observed concomitant crystallization in the presence of this additive, as observed in the crystallization experiments described in Section 3.3.1. The thermodynamic equilibrium point determined is 8 °C lower than that in pure water.

**Table 2.** Coefficients of the van't Hoff equation for solubility curves of 2,6MeOBA polymorphs in 1% aqueous solution of PEG.

Polymorph	a	b	R <sup>2</sup>	SE for lnS <sub>calc</sub>
I + PEG	−3910 ± 150	14 ± 0.5	0.9885	0.08
III + PEG	−3180 ± 200	12 ± 0.6	0.9698	0.12

Slurry-bridging experiments in the presence of PEG and HPC additives led to the same conclusions as those performed in pure water and toluene (see Section 3.1.2); after 24 h, the pure form I was obtained at 25, 50, and 70 °C, while at 80 °C, pure form III was obtained.

Using both additives, the results of the SMPT kinetic experiments were almost identical to those of the pure solvents (see Figure 6). In the presence of 1% PEG, the SMPT time of the 1:1 mixture of both polymorphs is the same as in pure solvents (less than 15 min), but 0.1% HPC decelerates the SMPT to form I at 25 °C, as the SMPT time in the presence of HPC is between 30 and 45 min. The time of SMPT from pure form III in the presence of 1% PEG is longer (between 30 and 45 min) than from the mixture of both polymorphs, but the addition of 0.1% HPC inhibited the SMPT of pure form III to form I. SMPT was not detected by sample slurring for 24 h. It is likely that PEG and HPC interact with the carboxyl group of 2,6MeOBA and stabilize the *syn* configuration in nucleation and inhibit the nucleation of form I.

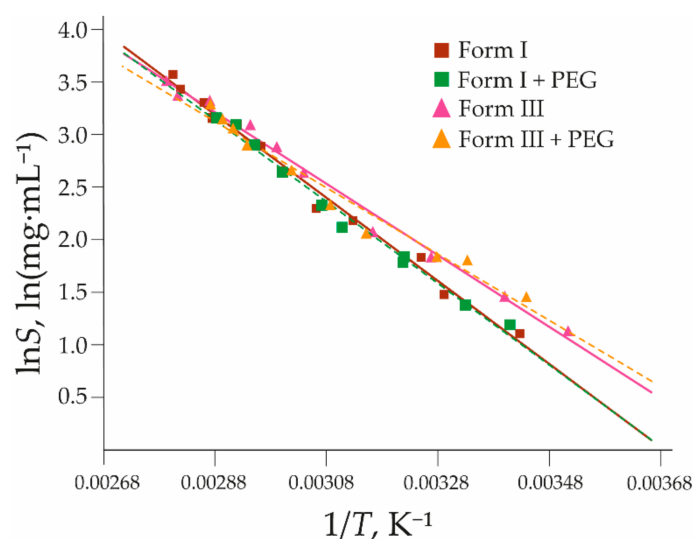


**Figure 9.** The solubility curves of 2,6MeOBA polymorphs I and III in pure water and 1% aqueous solution of PEG. Brown solid line—form I in pure water; Green dashed line—form I in 1% PEG solution; Magenta solid line—form III in pure water; Orange dashed line—form III in a 1% PEG solution. Triangles and squares represent the experimental data (see Supplementary Materials Tables S8 and S9); lines are calculated using Equation (1) with coefficients  $a$  and  $b$  found in the fitting using the least-squares approach, given in Table 2.

#### 4. Conclusions

The three previously reported polymorphs of 2,6MeOBA can be crystallized using different crystallization methods. Thermodynamic stability determined based on solvent-mediated phase transformations and solubility data shows that form III is stable at temperatures above 79 °C, whereas form I is thermodynamically stable at lower temperatures. The solvent-mediated phase transition from metastable to thermodynamically stable 2,6MeOBA polymorphs is very fast (less than 15 min at 25 °C and high stirring rates), which could explain why the preparation of metastable 2,6MeOBA polymorphs II and III is challenging.

The cooling rate and supersaturation are among the main variables that change the possibility of obtaining metastable polymorphs of 2,6MeOBA. Form III can be crystallized from water using a slow cooling rate and a fast stirring rate. Crystallization additives were shown to be able to improve the control of the crystallization polymorphic outcome, allowing nucleation for the pure metastable polymorph and decelerating the solvent-mediated phase transition rate by inhibiting the nucleation of the thermodynamically stable form. HPC can be used to slow the phase transition of form III to form I, although it cannot selectively provide the nucleation of only pure form III. PEG can be used to increase the probability of crystallization of metastable polymorphs of 2,6MeOBA.

**Supplementary Materials:** The following supporting information can be downloaded at: <https://www.mdpi.com/article/10.3390/cryst12081161/s1>, Table S1: List of additives used in the study; Figure S1: Phase identification of 2,6MeOBA polymorphs using PXRD patterns simulated from crystal structures deposited in the CSD; Table S2: Experimental solubility data for form I in water and coefficients  $a$  and  $b$  found in the fitting using the least-squares approach; Table S3: Experimental solubility data for form III in water and coefficients  $a$  and  $b$  of Equation (1) found in the fitting using the least-squares approach; Table S4: Detailed results from the crystallization of pure solvents and phase compositions of mixtures from the Rietveld analysis; Figure S2: Example of Rietveld refinement from Profex 4.3.6.; Table S5: Detailed results from the crystallization with additive presence and quantification results of mixtures from the Rietveld refinement; Table S6: Detailed results from the crystallization experiments from highly concentrated water solutions using different additives and cooling rates with quantification results of mixtures from the Rietveld analysis; Table S7: Detailed results from the crystallization experiments with different amounts and cooling rates with quantification results of mixtures from the Rietveld analysis; Table S8: Experimental solubility data

for form I in 1% PEG water solution and coefficients a and b from Equation (1) found in the fitting using the least-squares approach; Table S9: Experimental solubility data for form III in 1% PEG water solution and coefficients a and b from Equation (1) found in the fitting using the least-squares approach.

**Author Contributions:** Investigation, writing—original draft preparation and visualization, A.S.; Conceptualization, methodology, and writing—review and editing, A.S. and A.B.; Supervision, A.B. All authors have read and agreed to the published version of the manuscript.

**Funding:** This research was funded by European Social fund and Latvian state budget project “Strengthening of the capacity of doctoral studies at the University of Latvia within the framework of the new doctoral model”, identification No. 8.2.2.0/20/1/006.

**Institutional Review Board Statement:** Not applicable.

**Informed Consent Statement:** Not applicable.

**Data Availability Statement:** No new data were created or analyzed in this study. Data sharing is not applicable to this article.

**Conflicts of Interest:** The authors declare that they have no conflict of interest.

## Abbreviations

PVC—polyvinyl chloride; Poly 80—polysorbate 80; OGP—octyl  $\beta$ -D-glucopyranoside; PCL—polycaprolactone; PEG—polyethylene glycol; PheBorA—phenylboronic acid; 2,6MeOPheBorA—2,6-dimethoxyphenylboronic acid; HPC—hydroxypropyl cellulose; PAA—poly(acrylic amide); 4IPheBorA—4-iodophenylboronic acid; BIS-TRIS—bis(2-hydroxyethyl)amino-tris-(hydroxymethyl) methane; CA—cellulose acetate; PAS—poly-(acrylic acid); MCC—microcrystalline cellulose; 4COOHPheBorA—4-carboxyphenylboronic acid; Na CMC—sodium carboxymethyl cellulose; HPMC—hydroxypropylmethyl cellulose.

## References

1. Aitipamula, S.; Nangia, A. Polymorphism: Fundamentals and Applications. In *Supramolecular Chemistry*; John Wiley & Sons, Ltd.: Chichester, UK, 2012; ISBN 9780470661345.
2. Hilfiker, R. *Polymorphism: In the Pharmaceutical Industry*; Hilfiker, R., Ed.; Wiley-VCH Verlag GmbH & Co. KGaA: Weinheim, Germany, 2006; ISBN 9783527311460.
3. Fabbiani, F.P.A.; Allan, D.R.; Parsons, S.; Pulham, C.R. An Exploration of the Polymorphism of Piracetam Using High Pressure. *CrystEngComm* **2005**, *7*, 179–186. [[CrossRef](#)]
4. Karpinski, P.H. Polymorphism of Active Pharmaceutical Ingredients. *Chem. Eng. Technol.* **2006**, *29*, 233–237. [[CrossRef](#)]
5. Lu, J.; Rohani, S. Polymorphism and Crystallization of Active Pharmaceutical Ingredients (APIs). *Curr. Med. Chem.* **2009**, *16*, 884–905. [[CrossRef](#)]
6. Tandon, R.; Tandon, N.; Thapar, R.K. Patenting of Polymorphs. *Pharm. Pat. Anal.* **2018**, *7*, 59–63. [[CrossRef](#)] [[PubMed](#)]
7. Rakoczy, W.A.; Mazzochi, D.M. The Case of the Disappearing Polymorph: “Inherent Anticipation” and the Impact of SmithKline Beecham Corp. v Apotex Corp. (Paxil®) on Patent Validity and Infringement by Inevitable Conversion. *J. Generic Med.* **2006**, *3*, 131–139. [[CrossRef](#)]
8. Snider, D.A.; Addicks, W.; Owens, W. Polymorphism in Generic Drug Product Development. *Adv. Drug Deliv. Rev.* **2004**, *56*, 391–395. [[CrossRef](#)]
9. Pudipeddi, M.; Serajuddin, A.T.M. Trends in Solubility of Polymorphs. *J. Pharm. Sci.* **2005**, *94*, 929–939. [[CrossRef](#)] [[PubMed](#)]
10. De Tros Ilarduya, M.C.; Martín, C.; Goñi, M.M.; Martínez-Uhárriez, M.C. Dissolution Rate of Polymorphs and Two New Pseudopolymorphs of Sulindac. *Drug Dev. Ind. Pharm.* **1997**, *23*, 1095–1098. [[CrossRef](#)]
11. Gu, C.H.; Grant, D.J.W. Estimating the Relative Stability of Polymorphs and Hydrates from Heats of Solution and Solubility Data. *J. Pharm. Sci.* **2001**, *90*, 1277–1287. [[CrossRef](#)] [[PubMed](#)]
12. Vippagunta, S.R.; Brittain, H.G.; Grant, D.J.W. Crystalline Solids. *Adv. Drug Deliv. Rev.* **2001**, *48*, 3–26. [[CrossRef](#)]
13. Gupta, S.; Kesarla, R.; Omri, A. Formulation Strategies to Improve the Bioavailability of Poorly Absorbed Drugs with Special Emphasis on Self-Emulsifying Systems. *ISRN Pharm.* **2013**, *2013*, 848043. [[CrossRef](#)] [[PubMed](#)]
14. Bauer, J.; Spanton, S.; Henry, R.; Quick, J.; Dziki, W.; Porter, W.; Morris, J. Ritonavir: An Extraordinary Example of Conformational Polymorphism. *Pharm. Res.* **2001**, *18*, 859–866. [[CrossRef](#)] [[PubMed](#)]
15. Aguiar, A.J.; Krc, J.; Kinkel, A.W.; Samyn, J.C. Effect of Polymorphism on the Absorption of Chloramphenicol from Chloramphenicol Palmitate. *J. Pharm. Sci.* **1967**, *56*, 847–853. [[CrossRef](#)] [[PubMed](#)]

16. Singhal, D.; Curatolo, W. Drug Polymorphism and Dosage Form Design: A Practical Perspective. *Adv. Drug Deliv. Rev.* **2004**, *56*, 335–347. [[CrossRef](#)] [[PubMed](#)]
17. Censi, R.; Martino, P. di Polymorph Impact on the Bioavailability and Stability of Poorly Soluble Drugs. *Molecules* **2015**, *20*, 18759–18776. [[CrossRef](#)] [[PubMed](#)]
18. Tang, W.; Sima, A.D.; Gong, J.; Wang, J.; Li, T. Kinetic Difference between Concomitant Polymorphism and Solvent-Mediated Phase Transformation: A Case of Tolfenamic Acid. *Cryst. Growth Des.* **2020**, *20*, 1779–1788. [[CrossRef](#)]
19. Su, Y.; Xu, J.; Shi, Q.; Yu, L.; Cai, T. Polymorphism of Griseofulvin: Concomitant Crystallization from the Melt and a Single Crystal Structure of a Metastable Polymorph with Anomalously Large Thermal Expansion. *Chem. Commun.* **2018**, *54*, 358–361. [[CrossRef](#)]
20. Du, W.; Yin, Q.; Bao, Y.; Xie, C.; Hou, B.; Hao, H.; Chen, W.; Wang, J.; Gong, J. Concomitant Polymorphism of Prasugrel Hydrochloride in Reactive Crystallization. *Ind. Eng. Chem. Res.* **2013**, *52*, 16182–16189. [[CrossRef](#)]
21. Jiang, S.; ter Horst, J.H.; Jansens, P.J. Concomitant Polymorphism of O-Aminobenzoic Acid in Antisolvent Crystallization. *Cryst. Growth Des.* **2008**, *8*, 37–43. [[CrossRef](#)]
22. Munshi, P.; Venugopala, K.N.; Jayashree, B.S.; Guru Row, T.N. Concomitant Polymorphism in 3-Acetylcoumarin: Role of Weak C-H $\cdots$ O and C-H $\cdots$  $\pi$  Interactions. *Cryst. Growth Des.* **2004**, *4*, 1105–1107. [[CrossRef](#)]
23. Singh, A.; Lee, I.S.; Kim, K.; Myerson, A.S. Crystal Growth on Self-Assembled Monolayers. *CrystEngComm* **2011**, *13*, 24–32. [[CrossRef](#)]
24. Hernández Espinell, J.R.; López-Mejías, V.; Stelzer, T. Revealing Polymorphic Phase Transformations in Polymer-Based Hot Melt Extrusion Processes. *Cryst. Growth Des.* **2018**, *18*, 1995–2002. [[CrossRef](#)] [[PubMed](#)]
25. Svard, M.; Rasmuson, Å.C. M-Hydroxybenzoic Acid: Quantifying Thermodynamic Stability and Influence of Solvent on the Nucleation of a Polymorphic System. *Cryst. Growth Des.* **2013**, *13*, 1140–1152. [[CrossRef](#)]
26. Telford, R.; Seaton, C.C.; Clout, A.; Buanz, A.; Gaisford, S.; Williams, G.R.; Prior, T.J.; Okoye, C.H.; Munshi, T.; Scowen, I.J. Stabilisation of Metastable Polymorphs: The Case of Paracetamol Form III. *Chem. Commun.* **2016**, *52*, 12028–12031. [[CrossRef](#)] [[PubMed](#)]
27. Lee, E.H.; Byrn, S.R. Stabilization of Metastable Flufenamic Acid by Inclusion of Mefenamic Acid: Solid Solution or Epilayer? *J. Pharm. Sci.* **2010**, *99*, 4013–4022. [[CrossRef](#)] [[PubMed](#)]
28. Moshe, H.; Levi, G.; Mastai, Y. Polymorphism Stabilization by Crystal Adsorption on a Self-Assembled Monolayer. *CrystEngComm* **2013**, *15*, 9203–9209. [[CrossRef](#)]
29. Simone, E.; Steele, G.; Nagy, Z.K. Tailoring Crystal Shape and Polymorphism Using Combinations of Solvents and a Structurally Related Additive. *CrystEngComm* **2015**, *17*, 9370–9379. [[CrossRef](#)]
30. Song, R.Q.; Cölfen, H. Additive Controlled Crystallization. *CrystEngComm* **2011**, *13*, 1249–1276. [[CrossRef](#)]
31. Tulli, L.G.; Moridi, N.; Wang, W.; Helttunen, K.; Neuburger, M.; Vaknin, D.; Meier, W.; Shahgaldian, P. Polymorphism Control of an Active Pharmaceutical Ingredient beneath Calixarene-Based Langmuir Monolayers. *Chem. Commun.* **2014**, *50*, 3938–3940. [[CrossRef](#)] [[PubMed](#)]
32. Moridi, N.; Danylyuk, O.; Suwinska, K.; Shahgaldian, P. Monolayers of an Amphiphilic Para-Carboxy-Calix[4]Arene Act as Templates for the Crystallization of Acetaminophen. *J. Colloid Interface Sci.* **2012**, *377*, 450–455. [[CrossRef](#)] [[PubMed](#)]
33. Hiremath, R.; Basile, J.A.; Varney, S.W.; Swift, J.A. Controlling Molecular Crystal Polymorphism with Self-Assembled Monolayer Templates. *J. Am. Chem. Soc.* **2005**, *127*, 18321–18327. [[CrossRef](#)]
34. Hiremath, R.; Varney, S.W.; Swift, J.A. Selective Growth of a Less Stable Polymorph of 2-Iodo-4-Nitroaniline on a Self-Assembled Monolayer Template. *Chem. Commun.* **2004**, *23*, 2676–2677. [[CrossRef](#)] [[PubMed](#)]
35. Zhang, B.; Hou, X.; Dang, L.; Wei, H. Selective Polymorphic Crystal Growth on Self-Assembled Monolayer Using Molecular Modeling as an Assistant Method. *J. Cryst. Growth* **2019**, *518*, 81–88. [[CrossRef](#)]
36. López-Mejías, V.; Kampf, J.W.; Matzger, A.J. Nonamorphism in Flufenamic Acid and a New Record for a Polymorphic Compound with Solved Structures. *J. Am. Chem. Soc.* **2012**, *134*, 9872–9875. [[CrossRef](#)]
37. Simone, E.; Cenzato, M.V.; Nagy, Z.K. A Study on the Effect of the Polymeric Additive HPMC on Morphology and Polymorphism of Ortho-Aminobenzoic Acid Crystals. *J. Cryst. Growth* **2016**, *446*, 50–59. [[CrossRef](#)]
38. Caridi, A.; Kulkarni, S.A.; di Profio, G.; Curcio, E.; ter Horst, J.H. Template-Induced Nucleation of Isonicotinamide Polymorphs. *Cryst. Growth Des.* **2014**, *14*, 1135–1141. [[CrossRef](#)]
39. Watson, S.; Nie, M.; Wang, L.; Stokes, K. Challenges and Developments of Self-Assembled Monolayers and Polymer Brushes as a Green Lubrication Solution for Tribological Applications. *RSC Adv.* **2015**, *5*, 89698–89730. [[CrossRef](#)]
40. Rossi, A.; Savioli, A.; Bini, M.; Capsoni, D.; Massarotti, V.; Bettini, R.; Gazzaniga, A.; Sangalli, M.E.; Giordano, F. Solid-State Characterization of Paracetamol Metastable Polymorphs Formed in Binary Mixtures with Hydroxypropylmethylcellulose. *Thermochim. Acta* **2003**, *406*, 55–67. [[CrossRef](#)]
41. Parambil, J.V.; Poornachary, S.K.; Heng, J.Y.Y.; Tan, R.B.H. Template-Induced Nucleation for Controlling Crystal Polymorphism: From Molecular Mechanisms to Applications in Pharmaceutical Processing. *CrystEngComm* **2019**, *21*, 4122–4135. [[CrossRef](#)]
42. Bryan, R.F.; White, D.H. 2,6-Dimethoxybenzoic Acid. *Acta Crystallogr. Sect. B Struct. Crystallogr. Cryst. Chem.* **1982**, *38*, 1014–1016. [[CrossRef](#)]
43. Portalone, G. Redetermination of 2,6-Dimethoxy-Benzoic Acid. *Acta Crystallogr. Sect. E Struct. Rep. Online* **2009**, *65*, o327–o328. [[CrossRef](#)] [[PubMed](#)]

44. Portalone, G. A New Polymorph of 2,6-Dimethoxybenzoic Acid. *Acta Crystallogr. Sect. E Struct. Rep. Online* **2011**, *67*, o3394–o3395. [[CrossRef](#)] [[PubMed](#)]
45. Portalone, G. Crystal Structure and Hirshfeld Surface Analysis of a Third Polymorph of 2,6-Dimethoxybenzoic Acid. *Acta Crystallogr. Sect. E Crystallogr. Commun.* **2020**, *76*, 1823–1826. [[CrossRef](#)] [[PubMed](#)]
46. Pal, R.; Jelsch, C.; Malaspina, L.A.; Edwards, A.J.; Murshed, M.M.; Grabowsky, S. Syn and Anti Polymorphs of 2,6-Dimethoxy Benzoic Acid and Its Molecular and Ionic Cocrystals: Structural Analysis and Energetic Perspective. *J. Mol. Struct.* **2020**, *1221*, 128721. [[CrossRef](#)]
47. Bērziņš, A.; Semjonova, A.; Actiņš, A.; Salvalaglio, M. Speciation of Substituted Benzoic Acids in Solution: Evaluation of Spectroscopic and Computational Methods for the Identification of Associates and Their Role in Crystallization. *Cryst. Growth Des.* **2021**, *21*, 4823–4836. [[CrossRef](#)]
48. Brady, J.; Drig, T.; Lee, P.I.; Li, J.X. Polymer Properties and Characterization. In *Developing Solid Oral Dosage Forms: Pharmaceutical Theory and Practice*, 2nd ed.; Qiu, Y., Chen, Y., Zhang, G., Yu, L., Mantri, R.V., Eds.; Elsevier: Amsterdam, The Netherlands, 2017; pp. 181–223. ISBN 9780128024478.
49. Reus, M.A.; van der Heijden, A.E.D.M.; ter Horst, J.H. Solubility Determination from Clear Points upon Solvent Addition. *Org. Process Res. Dev.* **2015**, *19*, 1004–1011. [[CrossRef](#)]
50. Doebelin, N.; Kleeberg, R. Profex: A Graphical User Interface for the Rietveld Refinement Program BGMN. *J. Appl. Crystallogr.* **2015**, *48*, 1573–1580. [[CrossRef](#)]
51. Burger, A.; Ramberger, R. On the Polymorphism of Pharmaceuticals and Other Molecular Crystals. I. *Mikrochim. Acta* **1979**, *72*, 259–271. [[CrossRef](#)]
52. Ostwald, W. Studien Über Die Bildung Und Umwandlung Fester Körper. *Z. Phys. Chem.* **1897**, *22U*, 289–330. [[CrossRef](#)]
53. Datta, S.; Grant, D.J.W. Effect of Supersaturation on the Crystallization of Phenylbutazone Polymorphs. *Cryst. Res. Technol.* **2005**, *40*, 233–242. [[CrossRef](#)]
54. Liu, Y.; van den Berg, M.H.; Alexander, A.J. Supersaturation Dependence of Glycine Polymorphism Using Laser-Induced Nucleation, Sonocrystallization and Nucleation by Mechanical Shock. *Phys. Chem. Chem. Phys.* **2017**, *19*, 19386–19392. [[CrossRef](#)] [[PubMed](#)]
55. Lin, J.; Shi, P.; Wang, Y.; Wang, L.; Ma, Y.; Liu, F.; Wu, S.; Gong, J. Template Design Based on Molecular and Crystal Structure Similarity to Regulate Conformational Polymorphism Nucleation: The Case of  $\alpha,\omega$ -Alkanedicarboxylic Acids. *IUCr* **2021**, *8*, 814–822. [[CrossRef](#)] [[PubMed](#)]
56. Wu, H.; Wang, J.; Liu, Q.; Zong, S.; Tian, B.; Huang, X.; Wang, T.; Yin, Q.; Hao, H. Influences and the Mechanism of Additives on Intensifying Nucleation and Growth of P-Methylacetanilide. *Cryst. Growth Des.* **2020**, *20*, 973–983. [[CrossRef](#)]